

# Mechanism of 1,2-hydrate shift in some carbocations involved in steroid biosynthesis

---

Vrček, Valerije; Vinković Vrček, Ivana; Kronja, Olga

Source / Izvornik: *Croatica Chemica Acta*, 2001, 74, 801 - 813

Journal article, Published version

Rad u časopisu, Objavljena verzija rada (izdavačev PDF)

Permanent link / Trajna poveznica: <https://um.nsk.hr/um:nbn:hr:163:127588>

Rights / Prava: [In copyright](#) / [Zaštićeno autorskim pravom](#).

Download date / Datum preuzimanja: **2024-07-01**



Repository / Repozitorij:

[Repository of Faculty of Pharmacy and Biochemistry University of Zagreb](#)



## Mechanism of 1,2-Hydride Shift in Some Carbocations Involved in Steroid Biosynthesis

Valerije Vrček,\* Ivana Vinković Vrček, and Olga Kronja\*

Faculty of Pharmacy and Biochemistry, University of Zagreb,  
A. Kovačića 1, 10000 Zagreb, Croatia

Received April 9, 2001; revised June 21, 2001; accepted June 25, 2001

The mechanism of 1,2-hydride shift in protosteryl C(20) cation (**1A**) and in dammarenyl C(20) cation (**2A**) was investigated by the semi-empirical AM1 method and *ab initio* quantum chemical calculations (HF/3–21G level). Stationary points **1A/1B** and **2A/2B**, and the corresponding transition hydrido-bridged structures **1TS** and **2TS** were located on the energy surface. Process **1A**→**1B** turned out to be energetically more favorable than process **2A**→**2B** by *ca.* 9 kcal mol<sup>-1</sup>, mostly due to the unfavorable steric repulsive interaction between the methyl group at C(14) and the  $\beta$ -oriented side chain at C(17) in **1A** and the lack of CC-hyperconjugative stabilization in **1A**. The exothermicity of processes **1A**→**1B** and **2A**→**2B** was increased by subsequent introduction of substituents (H, Me, *i*-Pr, and *t*-Bu) at C(14). The more pronounced trend in **1A**→**1B** proves that the origin of the relative stability of **1B** comes from the steric interactions in **1A**. Introduction of the halogen atom (F, Cl, and Br), due to its -I effect and relatively small size, changed the direction of the equilibrium **1A<sub>Y</sub>/1B<sub>Y</sub>**, and **1A<sub>Y</sub>** was found to be by *ca.* 3 kcal mol<sup>-1</sup> more stable than **1B<sub>Y</sub>**.

*Key words:* steroid biosynthesis, quantum-chemical calculations, carbocations, hydride shift.

### INTRODUCTION

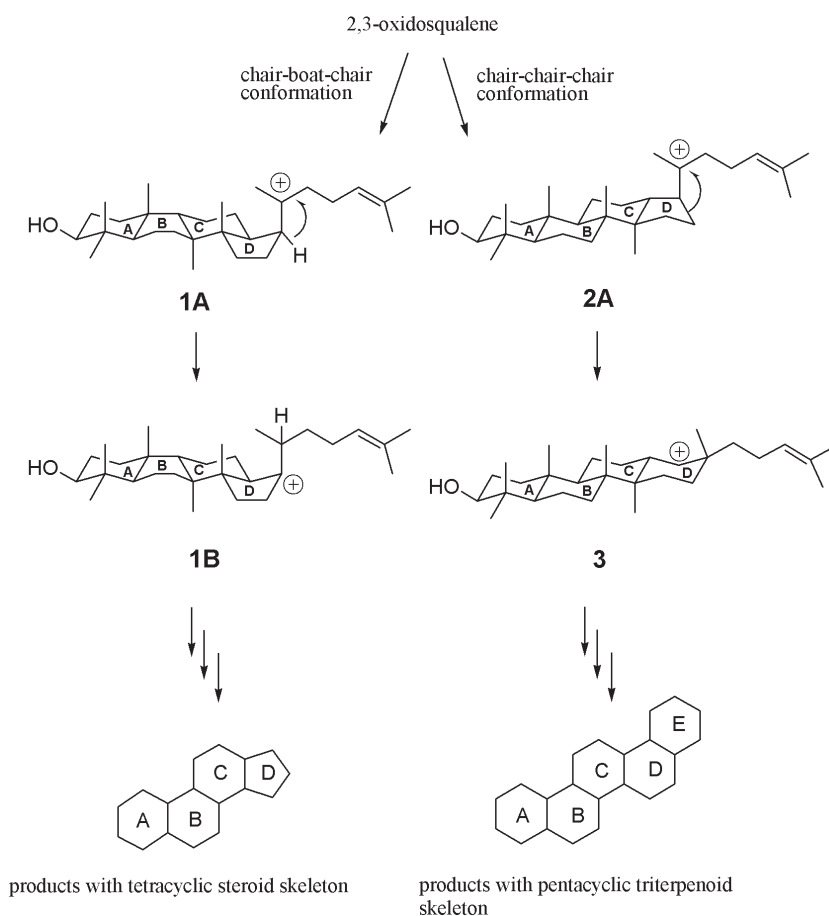
It has been established that the biological precursor of all steroids and polycyclic triterpenes is 2,3-oxidosqualene obtained by enzymatic oxidation

---

\* Author to whom correspondence should be addressed. (E-mail: V. V. – valerije@pharma.hr; O. K. – kronja@pharma.hr)

of squalene.<sup>1,2</sup> In animals, 2,3-oxidosqualene adopts the »chair-boat-chair« folding to generate the tetracyclic protosteryl C(20) cation (**1A**), the key intermediate step in the biosynthesis of lanosterol and all other steroid hormones, compounds with a tetracyclic structure having the five membered D ring (Scheme 1).<sup>3</sup> In plants, however, 2,3-oxidosqualene assumes a pre-chair conformation, yielding the tetracyclic dammarenyl C(20) cation (**2A**), which is the first »stopping point« in the biosynthesis of phytosterols, compounds with a pentacyclic structure having all six membered rings (Scheme 1).<sup>4</sup>

The first step in the cascade of rearrangements in the protosteryl cation **1A** is the 1,2-hydride shift from C(17) to C(20). In contrast, in the dammarenyl C(20) cation (**2A**), the key step in the series of rearrangements involves the expansion (Scheme 1) of the five membered D ring, *i.e.* migration



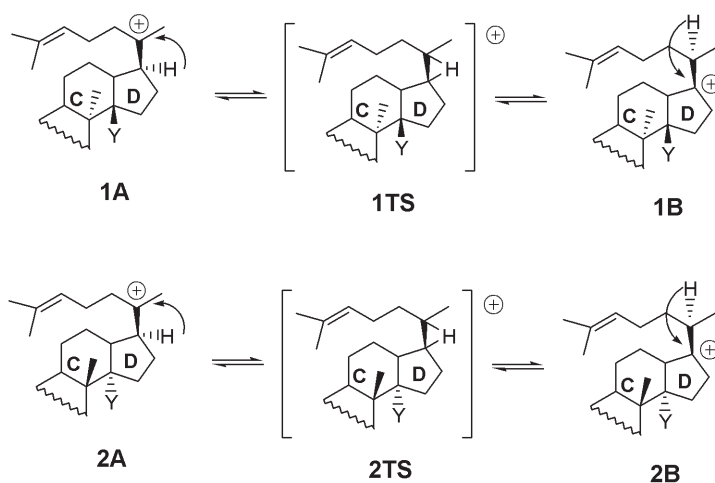
Scheme 1

of carbon. Thus, the apparent C(17)–C(20) hydride migration or its lack in the tetracyclic cation intermediates **1A** and **2A**, obtained after enzymatic cyclization of 2,3-oxidosqualene, is the crucial determinant of whether the subsequent rearrangements lead to formation of a tetracyclic steroid or pentacyclic triterpenoid skeleton (Scheme 1).

Corey and Virgil<sup>5</sup> postulated that the protosteryl C(20) cation (**1A**) is generated in the correct geometry for the C(17)–C(20) hydride migration, *i.e.* rotation of only 60° about the C(17)–C(20) bond is needed to facilitate the hydride shift. In the dammarenyl C(20) cation (**2A**), however, that angle is much larger, so the necessary rotation prior to the hydride migration is not favorable.

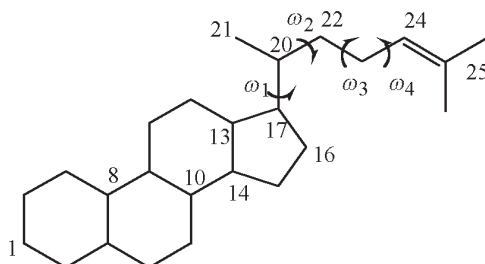
Experimental studies provide strong evidence that the pathway of rearrangement of **1A** is thermodynamically driven and requires minimum assistance from the enzyme.<sup>6</sup> Substrate analogue studies with the 2,3-oxidosqualene cyclases suggest that the enzyme's role during rearrangement is most probably simply to shield intermediate carbocations from addition of water or elimination by base, thereby allowing the hydride and methyl group migrations to proceed down a thermodynamically favorable and kinetically facile cascade.

In order to rationalize the striking difference in the rearrangements of the two isomeric carbocations, we set out to compare theoretically the 1,2-hydride shift rearrangements in protosteryl C(20) cation (**1A**) and in dammarenyl C(20) cation (**2A**) (Scheme 2), to describe the energy profiles of these processes, and to characterize the stationary points along the corre-



Scheme 2

sponding reaction pathways. In order to clarify the origin of the difference between the rearrangements that take place in cation **1A** and cation **2A**, particular emphasis was placed on studying how different substituents on C(14) affect the energetics of the hydride shift. Remote substituent effects of substituents located (steroid numbering defined in Scheme 3) on C(8), C(10), or C(1), were also investigated.



Scheme 3

Theoretical investigations of the model carbocation structures relevant to biomimetic polycyclization are rather scarce.<sup>7</sup> No quantum chemical calculations of the carbocation intermediates involved in steroid biosynthesis have been performed, except in the case of the protosteroyl cation which has been the subject of a molecular mechanics study.<sup>8</sup> Since complete application of a high-level *ab initio* method (e.g. MP $n$ ) is generally prohibitive in terms of computational effort for any but the smallest systems, in this paper we present combined semi-empirical and Hartree-Fock methods used for a systematic study of 1,2-hydride shifts in cations **1A** and **2A**. In particular, we will demonstrate that the semi-empirical AM1 method and *ab initio* Hartree-Fock (HF) level of theory with the 3–21G basis set can provide reasonable results for the carbocation structures which include subtle electronic and steric effects. We will also report the density function theory calculations (at the B3LYP/3–21G level) performed to estimate the electron correlation effects, which are critical for the accurate evaluation of carbocation relative energies.

## COMPUTATIONAL STUDIES

Quantum-chemical calculations were carried out with the Gaussian 94 program.<sup>9</sup> Full geometry optimizations of carbocation structures and frequency calculations were performed using the semi-empirical AM1 method,<sup>10</sup> and the *ab initio* Hartree-Fock (HF) level of theory with the 3–21G basis set.<sup>11</sup> Optimized AM1 and HF/3–31G

geometries were subjected to single point energy calculations at the B3LYP/3-21G level of theory.<sup>12</sup>

All stationary points were characterized as minima (no imaginary frequencies) or transition states (one imaginary frequency). The QST2 approach<sup>13</sup> was used to locate transition state structures, followed by examining the imaginary frequency's normal mode. Zero-point energies (ZPE) of the HF/3-21G geometries were scaled by 0.92.<sup>14</sup> The calculated energy barriers at the B3LYP/3-21G//AM1 level are comparable to the B3LYP/3-21G//HF/3-21G results (Table I). The relative energy differences obtained at the B3LYP/3-21G//AM1 and B3LYP/3-21G//HF/3-21G levels of theory are also similar (Table I). Thus, we found that the B3LYP/3-21G single point energy calculation based on the AM1 optimized geometry (B3LYP/3-21G//AM1 method) was the best compromise between speed and accuracy, and this approach was employed as a reference method to determine relative energy differences of carbocations throughout this work. This method was calibrated by comparison of the energetics of the 2-propyl-2-cyclopentyl/2-cyclopentyl-2-propyl model system<sup>15</sup> calculated at the B3LYP/6-31G(d)//B3LYP/6-31G(d) level of theory. The results obtained both for relative stabilities of carbocations and the calculated energy barriers are in close agreement, demonstrating the reasonable accuracy of the B3LYP/3-21G//AM1 method.

The conformation of the freely rotating C(17)-side chain was optimized by varying the torsion angles  $\omega_i$  (Scheme 3) between 0 and 360° in 30° increments. The rotamer having minimum energy calculated by the AM1 method was selected and used for calculations of relative energy differences between the corresponding carbocations.

## RESULTS AND DISCUSSION

### *Mechanism of 1,2-Hydride Shifts*

In protosteryl C(20) cation, which undergoes a C(17)–C(20) hydride migration, two minima, **1A** and **1B**, and an unsymmetrical hydrido-bridged transition state structure **1TS** were located on the energy surface (Figure 1).

The relatively high imaginary frequency (898i cm<sup>-1</sup>) corresponds to the hydride perturbation between C(20) and C(17) carbon atoms in the transition structure **1TS**.

At the B3LYP/3-21//AM1 level of theory, the calculated activation energy (Table I) for the reaction **1A**→**1B** is *ca.* 20 kcal mol<sup>-1</sup> (21 kcal mol<sup>-1</sup> at the B3LYP/3-21//HF/3-21G level), while the overall reaction is exothermic by *ca.* 9 kcal mol<sup>-1</sup> (10 kcal mol<sup>-1</sup> at the B3LYP/3-21//HF/3-21G level). The C(20)–C(22) bond in the minimum structure **1B** has the orientation that enables  $\beta$ -CC hyperconjugation with the formally empty 2p orbital on a carbocation center (Figure 1, hyperconjugative bond shown in black), since the dihedral angle between the empty p-orbital and the C(22)–C(20) bond in **1B** is about 4°. Therefore, the C(20)–C(22) bond in **1B** is elongated, and the corresponding C(22)–C(20)–C(17) angle is decreased (103°). In contrast, the spe-

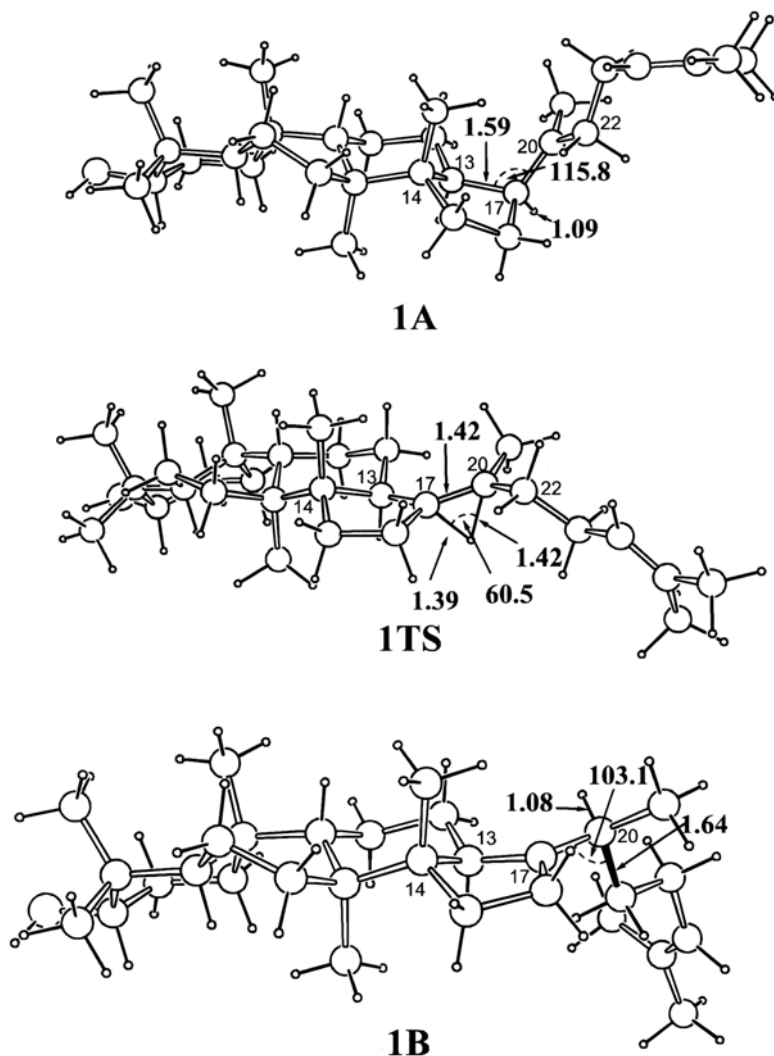


Figure 1. HF/3-21G optimized geometries of protosteryl C(20) cation (**1A**), protosteryl C(17) cation (**1B**) and the transition state structure **1TS**. Selected bond lengths are in angstroms and bond angles are in degrees.

cific feature of the minimum structure **1A** is the considerably increased C(13)–C(17)–C(20) bond angle ( $116^\circ$ ) caused by unfavorable repulsive interactions of the methyl group at C(14) position with the bulky *cis*-C(17)-side chain. As a consequence of this interaction, no hyperconjugative interaction with any CC bonds adjacent to the carbocation center occurs. These observations are in line with the large difference in energies of the two energy mini-

TABLE I

Relative energy differences calculated for protosteryl carbocations **1A** and **1B**, the transition state structure **1TS** and their C(14)-substituted derivatives **1A<sub>Y</sub>**, **1B<sub>Y</sub>**, and **1TS<sub>Y</sub>**, respectively

C(14)-Y	cation	$\Delta E/\text{kcal mol}^{-1}$	
		B3LYP/3-21G//AM1	B3LYP/3-21G//HF/3-21G
H	<b>1A<sub>Y</sub></b>	0	0
	<b>1TS<sub>Y</sub></b>	17.3	19.5
	<b>1B<sub>Y</sub></b>	-3.4	-4.5
Me	<b>1A</b>	0	0
	<b>1TS</b>	19.9	21.0
	<b>1B</b>	-8.9	-10.0
i-Pr	<b>1A<sub>Y</sub></b>	0	0
	<b>1TS<sub>Y</sub></b>	24.1	23.7
	<b>1B<sub>Y</sub></b>	-13.0	-12.7
<i>t</i> -Bu	<b>1A<sub>Y</sub></b>	0	0
	<b>1TS<sub>Y</sub></b>	26.3	33.2
	<b>1B<sub>Y</sub></b>	-19.9	-19.3
F	<b>1A<sub>Y</sub></b>	0	0
	<b>1TS<sub>Y</sub></b>	20.1	26.5
	<b>1B<sub>Y</sub></b>	2.4	8.3
Cl	<b>1A<sub>Y</sub></b>	0	0
	<b>1TS<sub>Y</sub></b>	21.3	23.7
	<b>1B<sub>Y</sub></b>	3.7	3.7
Br	<b>1A<sub>Y</sub></b>	0	0
	<b>1TS<sub>Y</sub></b>	15.2	17.0
	<b>1B<sub>Y</sub></b>	3.5	8.7

mum structures **1A** and **1B**, *i.e.* if the 1,2-hydride shift occurs yielding **1B**, unfavorable steric interaction is negligible, and the carbocation formed is stabilized by CC-hyperconjugation. From the reactant **1A** to the transition state **1TS**, the major structural changes are in that the C(17)-H bond distance increases from 1.09 Å to 1.39 Å, while the bond angle H-C(17)-C(20) decreases by 46° (Table II). The structure of the **1TS** is characterized by unsymmetrical C-H-C bridging (Figure 1). The corresponding C(20)-H bond distance in **1B** is 1.08 Å and the bond angle H-C(20)-C(17) is 109.6°.

In order to rationalize the apparent lack of the C(17)-C(20) hydride shift in the dammarenyl cation **2A**, we also simulated the **2A**→**2B** process theo-



TABLE II

Selected geometry parameters of **1A**, **1B**, **1TS**, **2A**, **2B** and **2TS** calculated at the HF/3–21G level of theory

Coordinate <sup>a</sup>	<b>1A</b>	<b>1TS</b>	<b>1B</b>	<b>2A</b>	<b>2TS</b>	<b>2B</b>
Bond lengths/ Å						
C(13)–C(17)	1.598	1.507	1.475	1.618	1.515	1.469
C(17)–C(20)	1.470	1.417	1.464	1.457	1.412	1.475
C(16)–C(17)	1.546	1.515	1.497	1.549	1.501	1.495
C(20)–C(22)	1.487	1.497	1.640	1.467	1.500	1.601
C(17)–H	1.091	1.397	–	1.082	1.460	–
C(20)–H	–	1.418	1.082	–	1.486	1.086
Bond angles/° and dihedral angles/°						
H–C(17)–C(20)	104.7	59.0	–	107.8	60.4	–
H–C(20)–C(17)	–	60.5	109.6	–	62.3	107.3
C(13)–C(17)–C(20)	115.8	129.0	125.9	107.2	124.7	127.2
C(17)–C(20)–C(22)	122.8	121.1	103.1	124.6	121.9	107.3
C(13)–C(17)–C(20)–2p	30.1	–	–	14.6	–	–
C(22)–C(20)–C(17)–2p	–	–	3.7	–	–	16.5

<sup>a</sup> Atom numbering defined in Scheme 3.

retically. As with the protosteryl cation **1A**, semi-empirical and *ab initio* calculations were carried out to locate the stationary points along the pathway **2A**→**2B** (Scheme 2) and to define the overall energy profile. The results, presented in Table III, show that C(17)→C(20) hydride shift in the dammarenyl C(20) cation (**2A**) is energetically a less favorable process (by *ca.* 9 kcal mol<sup>−1</sup> at the B3LYP/3–21G//AM1 level) than the corresponding 1,2-hydride shift in the protosteryl C(20) cation (**1A**). At the same level of theory, the energy barrier for the **2A**→**2B** process is 8 kcal mol<sup>−1</sup> lower than the corresponding energy barrier for the **1A**→**1B** process. The search for the transition state **2TS** connecting **2A** and **2B** isomers was performed by the QST2 method as described above. The structure of **2TS** is similar to the transition state **1TS** which connects **1A** and **1B** intermediates (Table II). The imaginary frequency (900i cm<sup>−1</sup>) is mainly associated with the hydride perturbation between C(20) and C(17) carbon atoms. The calculated geometries (Table II) of **2A** and **2B** are comparable to those found for **1A** and **1B**, respectively.

The important difference in the dammarenyl isomer is the position of the C(14)-methyl group which is *trans* relative to C(17)-side chain. Such an orientation does not result in unfavorable steric interactions between the C(14)-methyl group and C(17)-side chain which was found in the protosteryl

TABLE III

Relative energy differences calculated for dammarenyl carbocations **2A** and **2B**, the transition state structure **2TS** and their C(14)-substituted derivatives **2A<sub>Y</sub>**, **2B<sub>Y</sub>**, and **2TS<sub>Y</sub>**, respectively

C(14)-Y	cation	$\Delta E/\text{kcal mol}^{-1}$	
		B3LYP/3-21G//AM1	B3LYP/3-21G//HF/3-21G
H	<b>2A<sub>Y</sub></b>	0	0
	<b>2TS<sub>Y</sub></b>	12.9	13.0
	<b>2B<sub>Y</sub></b>	1.0	-2.8
Me	<b>2A</b>	0	0
	<b>2TS</b>	11.9	17.1
	<b>2B</b>	0.9	-2.8
i-Pr	<b>2A<sub>Y</sub></b>	0	0
	<b>2TS<sub>Y</sub></b>	15.1	15.4
	<b>2B<sub>Y</sub></b>	-4.2	-3.8
<i>t</i> -Bu	<b>2A<sub>Y</sub></b>	0	0
	<b>2TS<sub>Y</sub></b>	16.9	17.0
	<b>2B<sub>Y</sub></b>	-10.1	-9.3
F	<b>2A<sub>Y</sub></b>	0	0
	<b>2TS<sub>Y</sub></b>	12.9	14.4
	<b>2B<sub>Y</sub></b>	2.6	1.9
Cl	<b>2A<sub>Y</sub></b>	0	0
	<b>2TS<sub>Y</sub></b>	10.5	11.0
	<b>2B<sub>Y</sub></b>	2.2	0.9
Br	<b>2A<sub>Y</sub></b>	0	0
	<b>2TS<sub>Y</sub></b>	11.1	3.5
	<b>2B<sub>Y</sub></b>	1.7	-0.4

C(20) cation (**1A**). Dammarenyl C(20) cation (**2A**) can more readily align its C(13)–C(17) bond with the empty 2p orbital. This is not the case of the protosteryl C(20) cation (**1A**) in which the lack of the effective  $\beta$ -CC hyperconjugation results in poorer stabilization of the positive charge. Therefore, since the gain in energy with the C(17)–C(20) hydride shift in protosteryl cation **1A** is about 10 kcal mol<sup>-1</sup>, the migration occurs and **1B** can be considered to be the carbocation from which all steroid hormones can be derived. On the other hand, the energy difference between **2A** and **2B** is almost negligible, so the energetically more favorable ring expansion occurs, forming the six membered D ring (Scheme 1). This conclusion is in accord with the results

obtained with the 2-cyclopentyl-2-propyl cation, in which it was found that the ring expansion of the cyclopentyl ring, through the barrier of about 12 kcal mol<sup>-1</sup> ( $\Delta G^\ddagger$ , -120 °C), is energetically more favorable by about 5 kcal mol<sup>-1</sup> (at the B3LYP/6-31G(d) level) than the corresponding hydride migration process.<sup>15</sup> According to the results presented above, the preequilibrium process **2A**→**2B** may occur in the dammarenyl cation. However, **2B** is not observed experimentally, since the rearrangement products can be derived from **2A** only.

### *The Effect of Substituents on 1,2-Hydride Shift*

It is well known that substituent effects on reactive intermediates, such as carbocations, are often much larger than the analogous effects on neutral molecules.<sup>16</sup> Semi-empirical methods have been successfully used to predict energy trends arising from alternative conformations of steroids or substituent effects in a qualitative or semi-quantitative way.<sup>17</sup> In order to test our assumption that the relative instability of **1A** in comparison with **1B** originates almost entirely from the unfavorable repulsive interaction between the methyl group at C(14) and the *cis*-located side chain at C(17), we studied the influence of different substituents at C(14) on the energy profiles of the C(17)–C(20) hydride shift.

The relative effects of the substituents located at C(14) on the energy changes in the minima and transition structures were studied systematically, both in the protosteryl cation and dammarenyl cation. Two types of substituents were introduced into molecules **1A/1B** and **2A/2B**; the first group consists of alkyl groups increasing in size (H, Me, *i*-Pr, and *t*-Bu), and the other of halogen atoms (F, Cl, and Br). The effects of the C(14)-substituents on the relative stabilities of protosteryl cation derivatives **1A<sub>Y</sub>** and **1B<sub>Y</sub>** and the transition structures **1TS<sub>Y</sub>** (Y represents a given substituent at C(14) atom) are presented in Table I.

As expected, the thermodynamic feasibility of the process **1A<sub>Y</sub>**→**1B<sub>Y</sub>** increases with the increasing C(14)-alkyl group size. Thus, in the case of the C(14)-*tert*-butyl analogue **1A<sub>t-Bu</sub>**, the process **1A<sub>t-Bu</sub>**→**1B<sub>t-Bu</sub>** is 17 kcal mol<sup>-1</sup> (at the B3LYP/3-21G//AM1 level) more favourable than the corresponding process with the C(14)-hydrogen analogue (Table I). This is understandable, since **1A<sub>t-Bu</sub>** suffers the most from the unfavorable repulsive steric interactions of the bulky *tert*-butyl group with the  $\beta$ -C(17)-side chain. The best illustration of this interaction is the characteristic increase of C(13)–C(17)–C(20) bond angle in **1A<sub>Y</sub>** as the C(14) substituent size increases. Thus, in **1A<sub>H</sub>** that angle is 105°, in the protosteryl cation **1A** is 117°, while in **1A<sub>t-Bu</sub>** it is 126°. Even though the unfavorable steric interaction of the group located at C(14) and C(17)-side chain has the largest influence on the relative sta-

bility, other features of the structure also contribute to the overall energies. Thus, it is of interest to note that the  $\mathbf{1A}_{t\text{-Bu}}$  analog exists as a CH-hyperconjugative isomer, whereas the  $\mathbf{1A}_{\text{H}}$  analog is characterized by CC-hyperconjugative stabilization of the positive charge at C(17). On the other hand, the  $\mathbf{1B}_{\text{H}}$  analog exists as the CC-hyperconjugative isomer, and the  $\mathbf{1B}_{t\text{-Bu}}$  analog as the CH-hyperconjugative isomer. This is also a consequence of the strong repulsion of the groups located at C(14) and C(20), which prevents the more effective CC-hyperconjugative stabilization. The lack of CC-hyperconjugation in  $\mathbf{1A}_{t\text{-Bu}}$  drives the equilibrium even further toward  $\mathbf{1B}_{t\text{-Bu}}$ .

The trend of an increasing activation barrier with successive introduction of the C(14)-alkyl substituents (H, Me, *i*-Pr, *t*-Bu) for the process  $\mathbf{1A}_{\text{Y}} \rightarrow \mathbf{1B}_{\text{Y}}$  is obvious (Table I), but it is less pronounced than the substituent effect on the energy minimum structures. The predicted energy barriers for the process ranged from 17–26 kcal mol<sup>-1</sup> at the B3LYP/3–21G//AM1 level of theory.

We found a dramatic change in the  $\mathbf{1A}_{\text{Y}} \rightarrow \mathbf{1B}_{\text{Y}}$  process energetics when the halogen (F, Cl or Br) was introduced to C(14) position. The direction of the equilibrium  $\mathbf{1A}_{\text{Y}} / \mathbf{1B}_{\text{Y}}$  was changed, and  $\mathbf{1A}_{\text{Y}}$  was found to be *ca.* 3 kcal mol<sup>-1</sup> more stable than  $\mathbf{1B}_{\text{Y}}$  in all cases (Table I). These results can be attributed to both the steric and the electronic characteristics of the halogen. Unfavorable steric interactions are not present since the sizes of all halogen atoms are smaller than the alkyl substituents. The electronic interaction between the side chain and the halogen is more important, in which, because of the -I effect of the halogens, the  $\beta$ -orientation of the side chain is favorable. Somewhat unusually large energy barriers can be attributed to the inconsistency of both methods (AM1 and HF/3–21G) for predicting the correct transition state geometry, *i.e.* due to the lack of electron correlation in these theoretical models. Calculations with halogen substituents suggest that the equilibrium between the isomeric carbocations  $\mathbf{1A}$  and  $\mathbf{1B}$  can be readily shifted by selective placement of the appropriate substituent at C(14) position.

Similar effects are found in the case of the dammarenyl C(20) cation ( $\mathbf{2A}$ ) as for the protosteryl cation  $\mathbf{1A}$  with alkyl and halogen substituents at C(14). Even though the thermodynamic feasibility of the process  $\mathbf{2A}_{\text{Y}} \rightarrow \mathbf{2B}_{\text{Y}}$  increases with increasing the C(14)-substituent size, both the energy change (process  $\mathbf{2A}_{t\text{-Bu}} \rightarrow \mathbf{2B}_{t\text{-Bu}}$  is by *ca.* 10 kcal mol<sup>-1</sup> more favorable than process  $\mathbf{2A}_{\text{H}} \rightarrow \mathbf{2B}_{\text{H}}$ , Table III) and structural perturbations caused by C(14) substitution are less pronounced compared to those of the protosteryl cation. The C(14)-substituent in the dammarenyl C(20) cation  $\mathbf{2A}$  is *trans* with respect to the C(17)-side chain, which makes the steric interaction between the substituents less important.

To ascertain whether a substrate modification in the A, B, or C steroid rings could also perturb the energetics underlying the rearrangements described above, we investigated the effects of C(1), C(8) and C(10) substitutions (atom numbering defined in Scheme 3) on the relative stability of carbocations involved in steroid biosynthesis. Replacement of the C(1)-hydroxyl group by either halogen atom or alkyl group does not change the relative energy differences between **1A** and **1B**, or **2A** and **2B** intermediates, neither does it perturb the overall energy profile. However, introduction of different substituents at either C(8) or C(10) positions does alter the energetics of the investigated processes, although the effects are considerably smaller than the effects of C(14) substitutions. For example, the introduction of isopropyl or *tert*-butyl group at C(8) position in protosteryl cation reduces the exothermicity of the hydride shift reaction by 5 kcal mol<sup>-1</sup> and 4 kcal mol<sup>-1</sup>, respectively, in comparison with the **2A**→**2B** process, while substitution of the C(8) methyl with the hydrogen does not have any effect at all. In contrast, introduction of isopropyl or *tert*-butyl groups at the C(8) position in the dammarenyl cation did not cause any obvious change in the energy difference between the two corresponding energy minimum cations, while introduction of hydrogen favors the hydride shift process by *ca.* 7 kcal mol<sup>-1</sup> more than in **2A**→**2B**. These findings strongly suggest that computational simulations of steroid biosynthesis should not be limited to small model compounds only, but should be also performed with the full carbocation structures.

*Acknowledgement.* – We gratefully acknowledge financial support from the Ministry of Science and Technology of the Republic of Croatia (Grant No. 006151).

## REFERENCES

1. (a) L. Mulheirn, *J. Chem. Soc. Rev.* **1** (1972) 259–272. (b) I. Abe, M. Rohmer, and G. D. Prestwich, *Chem. Rev.* **93** (1993) 2189–2206.
2. (a) E. J. Corey, H. M. Cheng, C. H. Baker, S. P. T. Matsuda, D. Li, and X. Song, *J. Am. Chem. Soc.* **119** (1997) 1277–1288. (b) E. J. Corey, H. Cheng, C. H. Baker, S. P. T. Matsuda, D. Li, and X. Song, *J. Am. Chem. Soc.* **119** (1997) 1289–1296.
3. (a) E. E. van Tamelen, *J. Am. Chem. Soc.* **104** (1982) 6480–6481. (b) H. H. Rees, L. J. Goad, and T. W. Goodwin, *Biochem. J.* **107** (1968) 417–426.
4. T. W. Goodwin, in: J. W. Porter and S. L. Spurgeon (Eds.), *Biosynthesis of Isoprenoid Compounds*, Vol. 1, John Wiley, New York, 1980, pp. 443–480.
5. E. J. Corey and S. C. Virgil, *J. Am. Chem. Soc.* **113** (1991) 4025–4026.
6. E. J. Corey, S. C. Virgil, H. Cheng, C. H. Baker, S. P. T. Matsuda, V. Singh, and S. Sarshar, *J. Am. Chem. Soc.* **117** (1995) 11819–11820.
7. M. J. S. Dewar and C. H. Reynolds, *J. Am. Chem. Soc.* **106** (1984) 1744–1750.
8. C. Jenson and W. L. Jorgensen, *J. Am. Chem. Soc.* **119** (1997) 10846–10854.

9. M. J. Frisch, G. W. Trucks, H. B. Schlegel, P. M. W. Gill, B. G. Johnson, M. A. Robb, J. R. Cheeseman, T. Keith, G. A. Petersson, J. A. Montgomery, K. Raghavachari, M. A. Al-Laham, V. G. Zakrzewski, J. V. Ortiz, J. B. Foresman, J. Cioslowski, B. B. Stefanov, A. Nanayakkara, M. Challacombe, C. Y. Peng, P. Y. Ayala, W. Chen, M. W. Wong, J. L. Andres, E. S. Replogle, R. Gomperts, R. L. Martin, D. J. Fox, J. S. Binkley, D. J. Defrees, J. Baker, J. P. Stewart, M. Head-Gordon, C. Gonzalez, and J. A. Pople, *Gaussian 94*, Revision E.1, Gaussian, Inc., Pittsburgh PA, 1995.
10. M. J. S. Dewar, E. G. Zoebisch, E. F. Healy, and J. J. P. Stewart, *J. Am. Chem. Soc.* **107** (1985) 3902–3909.
11. (a) J. B. Collins, P. v. R. Schleyer, J. S. Binkley, and J. A. Pople, *J. Chem. Phys.* **64** (1976) 5142–5148. (b) M. S. Gordon, J. S. Binkley, J. A. Pople, W. J. Pietro, and W. J. Hehre, *J. Am. Chem. Soc.* **104** (1982) 2797–2801.
12. (a) A. D. Becke, *J. Chem. Phys.* **98** (1993) 5648–5652. (b) P. J. Stevens, F. J. Devlin, C. F. Chabrowski, and M. J. Frisch, *J. Chem. Phys.* **98** (1994) 11623–11627.
13. C. Peng and H. B. Schlegel, *Israel J. Chem.* **33** (1993) 449–454.
14. A. P. Scott and L. Radom, *J. Phys. Chem.* **100** (1996) 16505–16513.
15. V. Vrček, H.-U. Siehl, and O. Kronja, *J. Phys. Org. Chem.* **13** (2000) 616–619.
16. A. M. El-Nahas and T. Clark, *J. Org. Chem.* **60** (1995) 8023–8027.
17. (a) J. Ivanov, O. Mekenyan, S. P. Bradbury, and G. Schuurmann, *Quant. Struct.-Act. Relat.* **17** (1998) 437–449. (b) C. Kubligráficas, R. Vazquez, and J. Mendieta, *J. Mol. Struct.* **428** (1998) 189–194.

## SAŽETAK

### Mehanizam 1,2-hidridnog pomaka u nekim karbokationima uključanima u biosintezi steroida

Valerije Vrček, Ivana Vinković Vrček i Olga Kronja

Semiempirijskom metodom AM1, te *ab initio* kvantno-kemijskim računima (teorijska razina HF/3–21G) istraživana je mehanizam 1,2-hidridnog pomaka u protosterilnom C(20) kationu (**1A**) i damarenilnom C(20) kationu (**2A**). Na energijskoj plohi locirani su minimumi **1A/1B** and **2A/2B**, te vodikom premoštene prijelazne strukture **1TS** i **2TS**. Proces **1A**→**1B** energijski je povoljniji od procesa za 9 kcal/mol, zbog steričkog odbijanja metilne skupine smještene na C(14) i  $\beta$ -orijentiranog bočnog lanca smještenog na C(17), te zbog nepostojanja CC-hiperkonjugacije u **1A**. Uvođenjem rastućih alkilnih skupina (H, Me, *i*-Pr i *t*-Bu) u položaj C(14) primijećeno je povećanje egzotermnosti obaju procesa **1A**→**1B** i **2A**→**2B**. Veće povećanje egzotermnosti u procesu **1A**→**1B** upućuje na to da relativna stabilnost **1B** prema **1A** potječe od steričkih interakcija u **1A**. Uvođenjem atoma halogena (F, Cl, and Br), a zbog njegova -I efekta i relativno malog promjera, mijenja se smjer u ravnoteži između **1A<sub>Y</sub>**/**1B<sub>Y</sub>**, u kojoj je **1A<sub>Y</sub>** za oko 3 kcal mol<sup>-1</sup> stabilniji od **1B<sub>Y</sub>**.